Sustainable Energy, Grids and Networks 35 (2023) 101135

Contents lists available at ScienceDirect

Sustainable Energy, Grids and Networks

journal homepage: www.elsevier.com/locate/segan

Quantifying flexibility potential on district heating local thermal substations

Leonidas Zouloumis [a], Nikolaos Ploskas [b], Giorgos Panaras [a,*]

[a] Department of Mechanical Engineering, University of Western Macedonia, Kozani, Greece
[b] Department of Electrical and Computer Engineering, University of Western Macedonia, Kozani, Greece

A R T I C L E I N F O

Article history:
Received 29 April 2023
Received in revised form 19 June 2023
Accepted 2 August 2023
Available online 9 August 2023

Keywords:
District heating
Heating load peak-shaving
Thermal comfort
Smart control strategies
Thermal flexibility
Energy efficiency

A B S T R A C T

The current work investigates an integrated framework for evaluating DHN substation flexibility, which is commonly known to depend on thermal mass and controlling strategies. However, while it is already acknowledged that thermal comfort is a subjective and dynamic parameter, the present literature has not stressed out its contribution to DHN flexibility. Therefore, the aim of this study is to enrich the present flexibility potential evaluation methods, by considering three parameters for the evaluation of the substation flexibility potential: thermal mass, controlling strategies and thermal comfort settings. In this work the maximum thermal flexibility potential is set as the maximum thermal power reduction that the consumer can tolerate, without compromising thermal comfort. The building is simulated in multiparametric two-day simulation scenarios, where the thermal power cutoff event takes place during the second day. The current work has uncovered that by reducing the thermal comfort zone by 2 °C, the maximum power reduction increased from 15% to 17% for light buildings, and from 30% to 40% in heavy cases. Moreover, while implementing preheating controlling strategies lead to up to 60% maximum power reduction, considering the thermal comfort zone of the consumer could further increase the flexibility potential to 75% reduction and reduce preheating times. The methodology that emerges from this work could be used to increase the real-time adaptivity of DHN decision support systems based on evaluation, enhancement and exploitation of thermal network flexibility, as well as establish a bidirectional exchange of information between energy consumers and producers of the grid.

1. Introduction

1.1. State of the art

Over the recent years a need for reducing the energy consumption arises. This task has also emerged in the building sector, as it has been made aware that building energy consumption has a significant share on the EU primary energy consumption [1]. For the improvement of the energy management, a promising concept is the implementation of District Heating Network (DHN) systems. A DHN features a layout that enables the mass energy production and distribution to end-users (consumers), which provide economic benefits in more populated areas [2], while being economically viable to be facilitated at the same time [3,4]. Furthermore, the environmental prospects are a matter that is positively affected by the implementation of DHNs [5]. Recent generations of the DHNs (4th and 5th generation of DHNs) provide the potential addition of Renewable Energy Resources (RES) [6]. In addition, the reduction of their operating temperature levels can be achieved in the 5th generation, through the setup of locally installed heat pumps, that also ensure the personalized supply temperature demands is achieved [4]. Implemented numerical models that simulate 5th generation DHN operation point out that those networks could potentially operate at temperature levels close to ground temperature [7]. Moreover, the decentralization of the energy producers in the thermal grid is another benefit of the 4th and 5th generation DHNs [8]. On the other hand, DHNs face several challenges, such as the proper expansion of the grid and the addition of new consumers to it [9]. Also, by increasing the network size, phenomena such as the delayed heat propagation become an issue that affects the proper planning of heat demand provision [10]. Consequently, demand-side management has become a significant issue in thermal network management. Existing works implement demand-side methodology applications. Namely, the works of [11,12] Both apply demand-side management methodologies through user optimized heating load scheduling. As observed from those works, proper demand-side management is often paired with DHN flexibility.

* Corresponding author.
E-mail addresses: l.zouloumis@uowm.gr (L. Zouloumis), nploskas@uowm.gr (N. Ploskas), gpanaras@uowm.gr (G. Panaras).

https://doi.org/10.1016/j.segan.2023.101135
2352-4677/

Generally speaking regarding thermal systems, flexibility can be described as the ability of a system to change its operational load injection/extraction speed by exploiting the variable thermal system power and adaptability speed [13], as well as thermal capacity of buildings/network/storages [14]. In short, two thermal flexibility aspects are variable thermal system power and thermal storage. Multiple approaches to the definition and quantification of a system flexibility in the form of Performance Indicators (PI) have been used in the research community and were pointed out in various research reviews [15–17]. Using the above perceptions of thermal flexibility, research provides DHN demand-side management optimization propositions in the two aforementioned aspects.

The first flexibility aspect (i.e., thermal energy storage) examines the ability to exploit the heat delay propagation that, as already mentioned, manifests in DHNs and buildings-consumers. Contrary to the second aspect, this one seems to be a more popular subject of research, as far as the DHN flexibility scope is concerned. There is a multitude of approaches that investigate ways to enhance DHN flexibility by exploiting the thermal mass of the system, as well as point out system characteristics that directly affect it. The research of [18] suggests that utilizing the indoor environment of buildings and by extent, the thermal mass of the buildings, could lead to network power capacity requirement reduction. For example, it has been stated in [19] that key aspect of the building envelope characteristics that affect thermal system flexibility include thermal mass, insulation and air tightness. What is more, the study of [20] used the thermal capacity of the buildings to store produced electrical energy of building integrated photovoltaic (BIPV) system, so that building was cooled. In the events of efficiency reduction of the BIPV system, the cooling setpoint was increased. This allowed the exploitation of thermal flexibility in order to maximize the usage of the RES related electrical energy, while abstaining from drawing electricity from the grid. However, what was not investigated in that paper was the case of varying thermal comfort zones when applying the proposed methodology. In addition, thermal mass does not only exist in consumers, but also in the network itself. In the work of [21], flexibility of the DHN was enhanced by varying the heat flow of the DHN medium that is providing the heat loads to the consumers. It is noted that in this work the thermal comfort was evaluated by the observation frequency of low temperatures of the fluid that returns from the building-consumer. That means that there is the potential for this work to be reexamined, provided that building models are available, as well as thermal comfort zones are evaluated directly using temperatures from the building interior, and not from the temperature levels of the heating system. The work of [22] indicated that taking the thermal mass of the network into account may lead to cost and power curtailment.

Moreover, DHN flexibility not only depends on thermal capacity, but also the controlling strategies that are used in the network [14,17,22]. Control strategies can be correlated with the second flexibility aspect (thermal power variation). To start with, this aspect has been approached by research by managing the consumer heat load satisfaction by multiple sources, also known as multi-energy system optimization. More specifically, works examine the structures of such multi-energy systems, in terms of occupant thermal comfort [23], hydraulic operation [24], and even exergy assessment optimization [25]. It is worth mentioning that controlling strategy methodologies are a great tool for optimizing multi-energy system infrastructure [26].

A prime example of this are predictive control strategies in DHNs. In this context, several works manage to predict the state of the DHN system and therefore schedule the heating load and the network operation in advance. Actions like preheating, also used in studies [27,28], require that future states of the building are known, which is attainable by predictive controlling. Namely, the majority of studies utilize model predictive controlling (MPC), which is considered one the of the most effective predictive controlling layouts for DHN operation. More specifically, in [29], an MPC layout is used, along with a simplified physics model, capable of considering the consumer thermal mass in the thermal controlling. In another study [30], MPC is implemented to reduce the primary energy consumption in a centralized solar DHN system, using detailed models of the components of the network. Additionally, a decentralized controlling approach is applied by [31], where every building has its own MPC, which is responsible for determining the optimal heating demand. On the other hand, the thermal plant has also its own MPC, which attempts to minimize thermal production cost and concurrently meet the thermal demands of the consumers. In other words, this is an example of single-direction information transference from the controllers of the consumers to the controller of the producers. MPC has been also used for lowering the network temperature levels [32], as well as the configuration of the operation of pumps distributing the thermal load [33]. In general, MPC strategies can optimize DHN operation in real-time application, although it is required that an accurate enough representation of the real system is used as a simulation model, as also confirmed from the literature above.

Furthermore, other layouts, such as Reinforcement Learning [34], Genetic Algorithms [35] and Mixed Integer Linear Programming [36,37] can also be spotted in the literature, regarding optimized DHN operation and demand-side management. One major challenge that predictive controlling faces as a tool to manage heat loads of DHNs is that a reliable model of the existing system (the thermal grid, its subsystems and consumers) is vital to its effective use.

Regarding its utilization, flexibility is mostly associated with attempts to optimize heat load schedule, in terms of primary energy consumption. This is achieved by exploiting thermal grid flexibility to shave peak heating loads, by using the thermal masses present in the grid [38]. Peak loads have been reported to occur mostly after night setbacks [39]. Efforts to decrease the peak loads also include the implementation of load shifting in several works [40,41], while [28] has also investigated the concept of indoor air preheating as a load shifting method to decrease peak loads in DHN. The same study has also examined scenarios of variable indoor temperature setpoints, depending on heat load cost. This allowed the building to collect heating loads during low-cost phases and store them in order to attain the necessary thermal comfort during high-cost phases, leading to primary energy consumption reduction. Moreover, load shifting is an effective strategy for maintaining thermal comfort during imminent heat supply cut-off events [27]. Increasing flexibility and reducing the cost are directly linked in the case of district heating networks [42,43]. Lastly it should be noted that flexibility is an expendable resource when exploited and needs certain time periods to recover [44]. Since heating rescheduling leads to the reduction of peak loads, the current design of the heating systems in the thermal grid may lead to cases of over-dimensioning, and therefore optimal characteristics of the thermal system installed in the DHN should be reinvestigated. An instance of the required heating output being reduced due to rescheduling having been observed is in the work of [45].

Broadly speaking, the existing literature has identified mechanics that affect thermal system flexibility in district heating networks, as well as ways to increase the thermal flexibility by utilizing predictive controlling. However, in the presented cases above, occupant comfort is considered as a static optimization criterion. To elaborate, it has been widely established that thermal comfort is the most prevalent aspect of occupant comfort [46]. An emerging research concept regarding the system flexibility management in DHNs is the perception of occupant thermal comfort as a dynamic, variable, and subjective optimization parameter that influences thermal grid operation. Results of a parametric study of flexibility uncertainty [47] state that occupant thermal comfort is something that should be closely observed when evaluating DHN flexibility potential. Therefore, there are prospects for further evolving the methodologies used for evaluating the flexibility potential of the building. Current research focuses on evaluating flexibility potential using thermal mass and controlling strategies, whereas there is a need for including the thermal comfort settings of the consumers as a prime factor when assessing DHN flexibility.

1.2. Aim of this work

The purpose of this work is to propose an integrated methodology regarding the evaluation of a DHN substation flexibility potential during power output reduction periods, that either take place for peak-shaving purposes, or happen due to thermal power unexpected cut-down events. More specifically, the approach examines the maximum heating power reduction that the substation is able to withstand, without compromising the thermal comfort of the occupant-consumer.

Most works focus on evaluating the flexibility potential in respective thermal grid through the examination of two parameters that are known to affect the flexibility potential of a thermal network, namely controlling strategies and thermal mass. The proposition of this study, however, attempts to use those two parameters in combination with a third: the thermal comfort characteristics of the occupant. The addition of this third parameter, as shown by the literature may potentially provide a more dynamic perception to the evaluation flexibility potential, which is affected by the occupants as well. Therefore, the proposed approach addresses the following subjects:

- Consideration of the thermal comfort settings, along with the building thermal mass and implemented controlling strategies, in the assessment of the substation thermal flexibility. It is noted that the present literature has room for further examination of the combination of those three factors.
- Multi-parametric dynamic simulation scenarios of the substation and its building-consumer, during events of thermal power reduction, due to peak-shaving or power cutdown strategies. Those scenarios contain various instances of thermal comfort settings, building weight categories, as well as different controlling strategies. The inclusion of all those factors in the simulations provide a generalized result regarding the performance of the proposed methodology, namely the evaluation of the flexibility potential of the substation.

This methodology could be implemented in DHN decision support systems, regarding the dynamic demand-side management of the heating loads supported in the thermal network.

2. Materials and methods

2.1. General description

In this section, the implemented methodology for the estimation of the building thermal flexibility potential is analyzed. Afterwards, parameters that affect said flexibility are also examined. The methodology is summarized in the following list.

(1) Implementation of the simulation environment that will be used for the peak shaving potential analysis.
(2) Establishment of a valid building model, as well as validated district heating systems and components.
(3) Determination of the simulation scenarios that will be conducted, as well as the variable parameters whose influence in thermal flexibility of the substation will be examined.
(4) Generation of results and discussion on the observations, regarding the system thermal flexibility potential, as well as its connection on the examined parameters.

Since the aim of those simulations is the determination of substation thermal flexibility, an indicator should be used for the quantification of it. For the purpose of this work, the thermal flexibility potential of the substation is described as follows: the building reaches its maximum thermal flexibility potential, when the reduction of available heating power of primary loop is such, that thermal comfort is altered more than 5% (absolute value), when compared to the respective reference case scenario (namely the scenarios where no power reduction event exists). The system and its characteristics are elaborated in the next subsection, for clarification reasons.

2.2. Simulation case

As already explained, the case system is a DHN substation that provides heating loads to an office building (Fig. 2.1).

More specifically, it consists of several components, namely a thermohydraulic network responsible for providing heating in the building interior. The network is divided into a primary loop (left side) and a secondary loop (right side), which are indirectly connected through a heat exchanger. The primary loop is open-ended and receives heated flow from a supposed producer. The primary heated flow is controlled by a valve which operates accordingly, in order to heat the secondary loop fluid to the desired temperature setpoint. The heating energy is transferred through the heat exchanger to the secondary loop and heats the circulating fluid. Finally, the heated flow of the secondary loop, which is controlled by a building thermostat, is provided in the indoor air of the building conditioned zone through a radiator.

As far as the building is concerned, it is a $10 \times 10 \times 3.16$ m^3 box-shaped building, with a 5×2.12 m^2 window on the south wall and a 2 x 1 door on the eastern wall. It is noted that the building is exposed to climate conditions that correspond to those of Kozani, Greece, during January [48]. Therefore, the respective climatic data were used in the simulations. In addition, since in this simulation the thermal behavior of a building is examined, a user is going to occupy the building during the time period 08:00 - 17:00 (typical office working schedule).

2.3. Simulation components

For the purpose of this work, model libraries were developed in Python environment. More specifically those libraries fall under two main categories. The first is the library of the component models of the thermohydraulic network. The components are the heat exchanger and the radiator models, that derive from TRNSYS physical equations [49]. More specifically, for the heat exchanger, the following equations are used (Eqs. (1)–(4)).

$$C_{pr} = \dot{m}_{pr} \cdot C_{p,pr} \ [\frac{\mathrm{W}}{\mathrm{K}}] \tag{1}$$

$$C_{sec} = \dot{m}_{sec} \cdot C_{p,sec} \ [\frac{\mathrm{W}}{\mathrm{K}}] \tag{2}$$

$$\begin{cases} C_{min} = C_{pr}, & C_{pr} < C_{sec} \\ C_{min} = C_{sec}, & C_{pr} > C_{sec} \end{cases} \tag{3}$$

where:

C_{pr}: Thermal capacity of the primary loop fluid flow

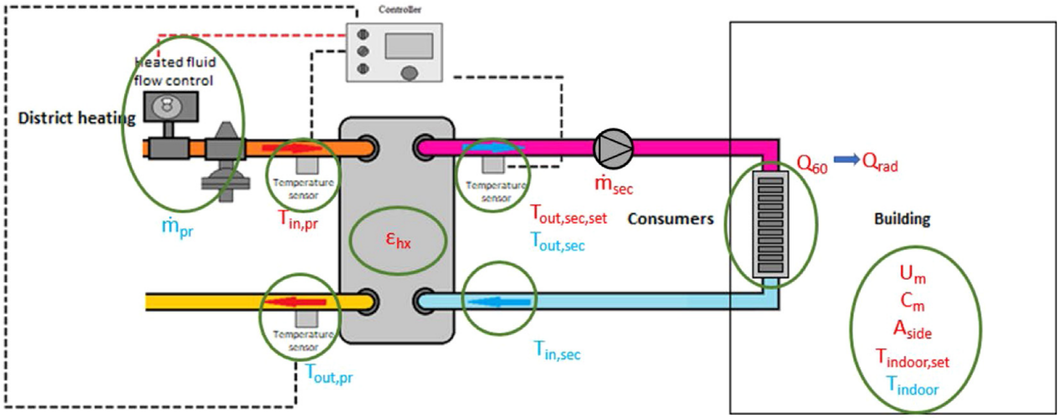

Fig. 2.1. Schematic representation of the simulated case of a district heating substation connected to a building.

C_{sec}: Thermal capacity of the secondary loop fluid flow
C_{min}: Minimum thermal capacity between both fluid flows
$\dot{m}_{pr}$: Primary loop fluid mass supply [kg/s]
$\dot{m}_{sec}$: Secondary loop fluid mass supply [kg/s]
$C_{p,pr}$: Primary loop fluid thermal capacity [J/(kg K)]
$C_{p,pr}$: Secondary loop fluid thermal capacity [J/(kg K)]

Maximum heat transfer $\dot{Q}_{max}$ depends on the minimum thermal capacity between both fluid flows C_{min} and the temperature difference between primary and secondary inlet flow (Eq. (4)).

$$\dot{Q}_{max} = C_{min} \cdot \left(T_{i,pr} - T_{i,sec}\right) \quad [\mathrm{W}] \tag{4}$$

where:

$T_{i,pr}$: Temperature of the primary loop fluid that enters the heat exchanger

$T_{i,sec}$: Temperature of the secondary loop fluid that enters the heat exchanger

Actual heat transfer is calculated in Eq. (5):

$$\dot{Q}_{ac} = \varepsilon \cdot \dot{Q}_{max} \quad [\mathrm{W}] \tag{5}$$

Finally, fluid temperatures exiting the heat exchanger are calculated in Eqs. (6) and (7):

$$T_{o,pr} = T_{i,pr} - \frac{\dot{Q}_{ac}}{C_{pr}} \quad [^{\circ}\mathrm{C}] \tag{6}$$

$$T_{o,sec} = T_{i,sec} - \frac{\dot{Q}_{ac}}{C_{sec}} \quad [^{\circ}\mathrm{C}] \tag{7}$$

where:

$T_{o,pr}$: Temperature of the primary loop fluid that exits the heat exchanger

$T_{o,sec}$: Temperature of the secondary loop fluid that exits the heat exchanger

As far as radiator heating power is concerned, the following equations take place for the calculations:

$$\dot{Q}_{rad} = \dot{Q}_{60} \cdot \left(\frac{\frac{T_{o,cons}+T_{o,cons}}{2} - T_{indoor}}{60}\right)^{1.33} \quad [\mathrm{W}] \tag{8}$$

$$T_{o,cons} = T_{i,cons} - \frac{\dot{Q}_{rad}}{\dot{m}_{sec} \cdot C_{sec}} \quad [^{\circ}\mathrm{C}] \tag{9}$$

where:

$T_{o,cons}$: Temperature of the secondary loop fluid that exits the radiator

$T_{i,cons}$: Temperature of the secondary loop fluid that enters the radiator [°C]

$\dot{m}_{sec}$: Secondary loop fluid mass supply [kg/s]

$\dot{Q}_{60}$: Radiator nominal operation heating power @60 °C active temperature [W]

T_{indoor}: Building indoor temperature [°C]

The second library category consists of the models that depict the thermal mechanics that occur in a building. Starting with the building model, it is based on the physical equations of the ISO 13790- simple hourly model [50]. More specifically, the building model in this method is a 5 resistance, 1 capacitance (5R1C), which has been proven to be sufficiently accurate in simulating building thermal mechanics on a daily basis [51]. Additionally, the building demand is calculated according to the simulation procedure of the building that was followed (see Section 2.4.). Despite it being an hourly model, the controlling systems act on regular intervals, affecting the indoor space and, hence, require that the simulation model runs at a sub-hourly time step. Furthermore, ISO 13790 - simple hourly model requires the evaluation of solar gains, which are calculated using local solar radiation data [48], according to the equations found in [52].

2.4. Simulation scenarios

In this section, the simulation scenarios that will take place in this work are presented. Each simulation lasts for two days and runs on a timestep of 1 min. During the first day, the district heating substation is going to operate as usual, while at the start of the second day and onwards, the substation is going to have a reduced ability to heat the building. In this case, this is achieved by reducing the maximum hot fluid flow in the primary loop. This in turn will reduce the energy that passes through the heat exchanger to the secondary loop and consequently, to the building. The purpose of the simulations is to examine how thermal comfort is affected at all scenarios. Through this observation, the thermal flexibility limits of the building are revealed, for each different scenario. In short, the building thermal flexibility evaluation is performed as follows:

1. Two-day simulation of the building for each scenario, without heat flow reduction (reference point scenarios)
2. Two-day simulation of the building for each scenario, with gradual heat flow reduction during the second day (reduced heat flow scenarios). The maximum heat flow reduction will be conducted, by restraining the maximum primary flow mass supply.
3. Comparison of the thermal comfort between scenarios
   The thermal comfort percentage (TCP) indicator is calculated according to Eq. (10):

$$\mathrm{TCP} = \frac{t_{comfort}}{t_{occupancy}} \quad [\%] \tag{10}$$

where:

Table 2.1
Fixed parameters of the substation used in the simulations.

Fixed parameters			
Symbol	Description	Value	Unit
$T_{in,pr}$	Heat exchanger, primary side inlet temperature	95	°C
$T_{out,sec,set}$	Heat Exchanger, secondary side outlet temperature setpoint	90	°C
U_m	Building average heat loss coefficient	0.7	W/(m^2 K)
A_{side}	Building total side area	344	m^2
$T_{indoor,set}$	Building indoor temperature setpoint	19	°C
ε_{hx}	Nominal heat exchanger effectiveness	0.9	–
$\dot{m}_{pr}$	Maximum primary loop mass supply	0.05	kg/s
$\dot{m}_{sec}$	Secondary loop mass supply	0.05	kg/s
Q_{60}	Radiator nominal operation heating power @60 °C active temperature	4000	W
ε_{rad}	Nominal radiator effectiveness	1	–

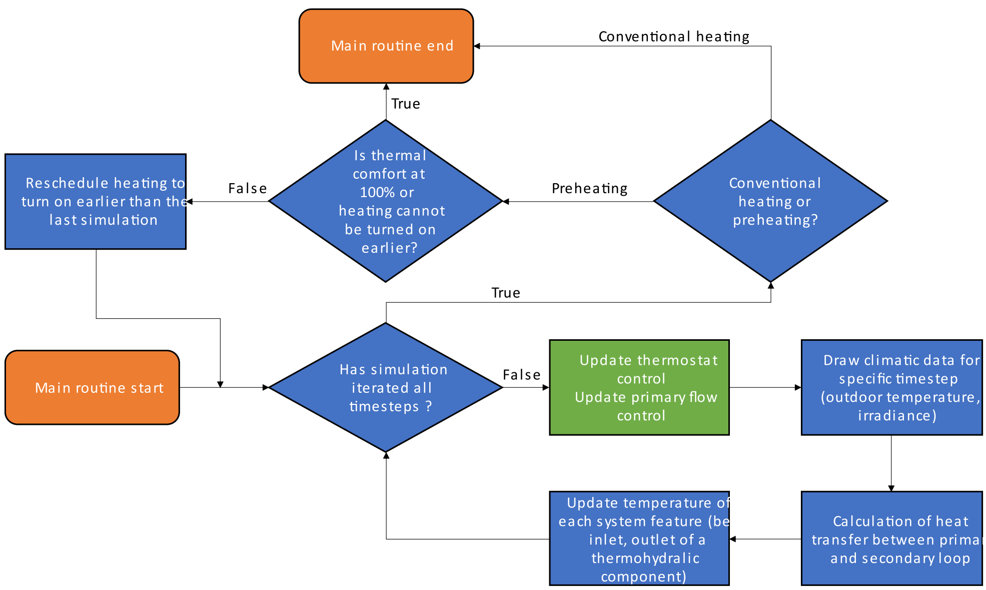

Fig. 2.2. Flow graph of the simulation procedure, implementing the controlling strategies.

$t_{comfort}$: Time that elapsed, where the indoor temperature did not fall below the bottom limit of the respective thermal comfort zone during occupancy
$t_{occupancy}$: Time that elapsed during the occupancy period

4. Evaluation of thermal flexibility potential (maximum heat flow reduction without compromising reference point thermal comfort levels)
   At this point, the parameter values that are taking place during the simulations are displayed. First of all, the fixed parameters that are used in all simulation are presented in Table 2.1.

Furthermore, simulations cover each combination of the following scenario features, whose characteristics are elaborated below (see Table 2.2). Moreover, those parameters will be examined for two different controlling strategies that the substation will adopt, namely conventional heating and preheating strategy [53] (Fig. 2.2).

Finally, it should be noted that the indoor air temperature is uniform across the interior space. In addition, the space is always heated using the conventional heating strategy during the occupancy hours for the first day of the two-day simulation. However, energy consumption and thermal comfort are not taken into account in the final results, regarding the first day of each simulation. Essentially, the focus is placed on the second day of each simulation.

3. Results

3.1. General information on dynamic simulations

Before the scenario results are presented, in order to grasp the heat power output energy reduction in a more practical sense, the heat power output reduction correlated to primary loop mass supply reduction is presented in Fig. 3.1, which applies both in conventional and preheating thermostat cases.

As it can be seen from Fig. 3.1, heating power output of the substation is reduced at significant rates when mass supply is reduced. More specifically, max substation power output reaches 1 kW (75% reduction) at 90% primary loop mass supply reduction. It can be seen that the correlation between mass supply curtailment of the primary loop and the thermal power reduction of the substation are correlated almost linearly.

Moreover, in Figs. 3.2–3.5 a case of a two-day simulation is presented, where 90% primary loop mass supply reduction takes place in the second day of the simulation.

As Figs. 3.2 and 3.3 display, during the first day of the simulation, the building operates in a business-as-usual schedule. However, during the second day, a thermal power supply reduction occurs, which could originate from a peak-shaving, or merely an unexpected cut-down event. During the second day, the mass supply, and consequently, the thermal load output of the substation to the building is significantly reduced in the case of Fig. 3.1 (75% power reduction). Additionally, the mass supply curtailment eventually led to low return temperatures of the primary loop

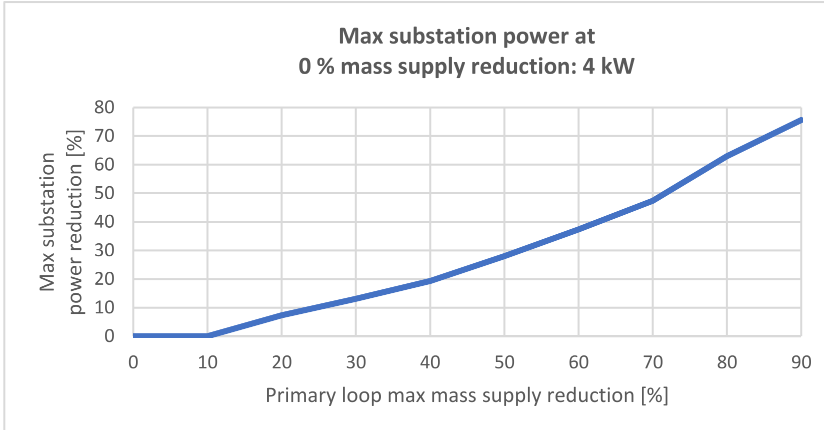

Fig. 3.1. Thermal comfort results for the second simulation day for all conventional heating scenarios.

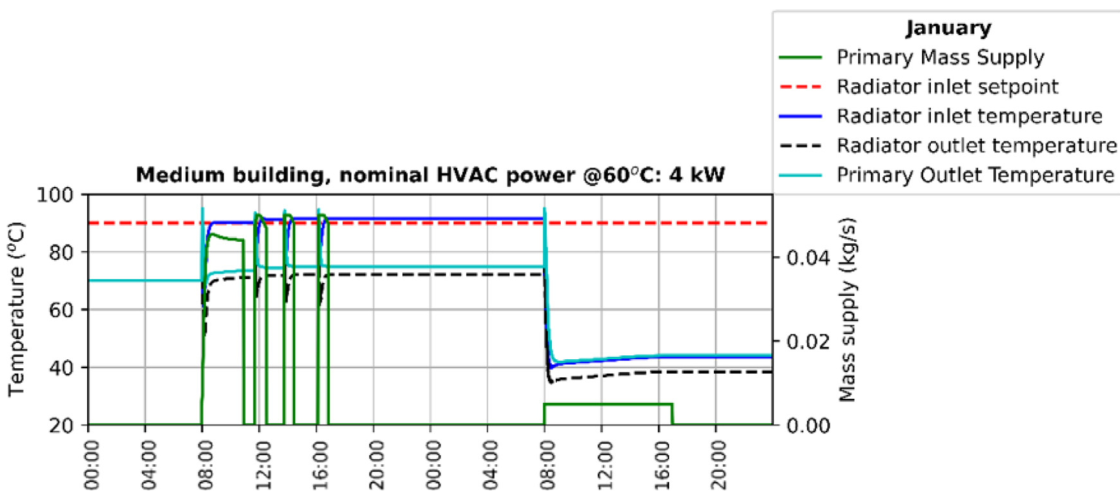

Fig. 3.2. Example of a two-day simulation scenario (temperatures and mass supply results of the substation).

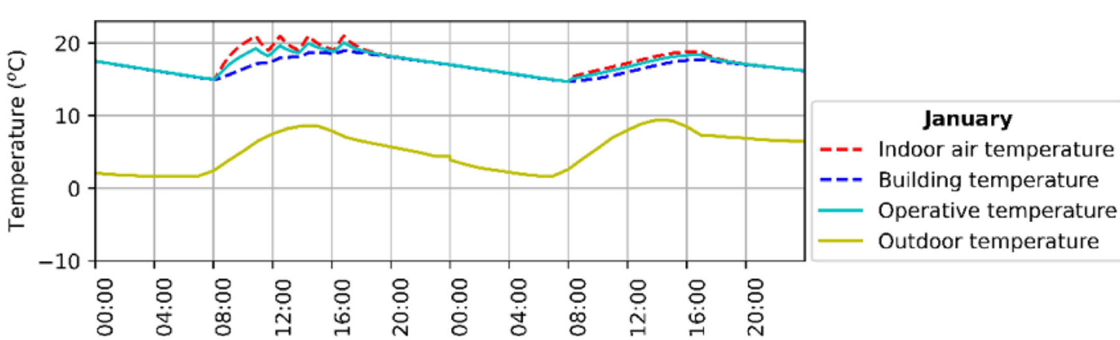

Fig. 3.3. Example of a two-day simulation scenario (building temperatures).

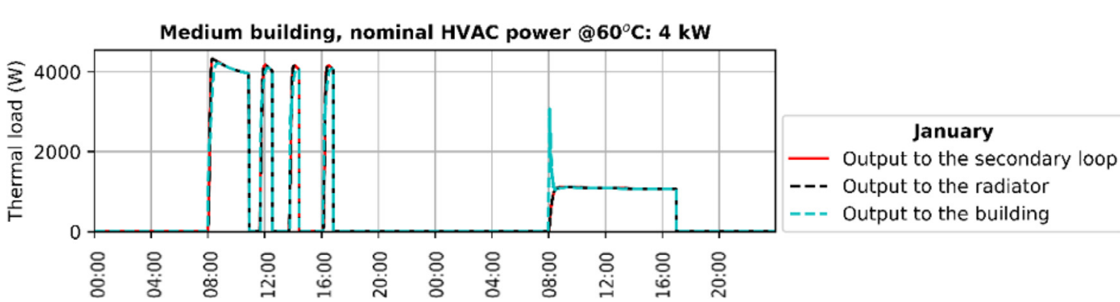

Fig. 3.4. Example of a two-day simulation scenario (thermal energy results of the substation).

Table 2.2
Scenario parameters that are used in the simulations.

Scenario parameters			
Symbol	Description	Value	Unit
C_m	Building heat capacity	80 000 (Very light) 165 000 (Medium) 360 000 (Very heavy)	J/K
R_m	Maximum primary loop mass supply reduction	0–90 (0 is considered the reference case for each scenario)	%
T_{comf_range}	Indoor air temperature comfort range of the occupant	20–22 19–21 (1 °C decrease of the first temperature range case) 18–20 (1 °C decrease of the first temperature range case)	°C

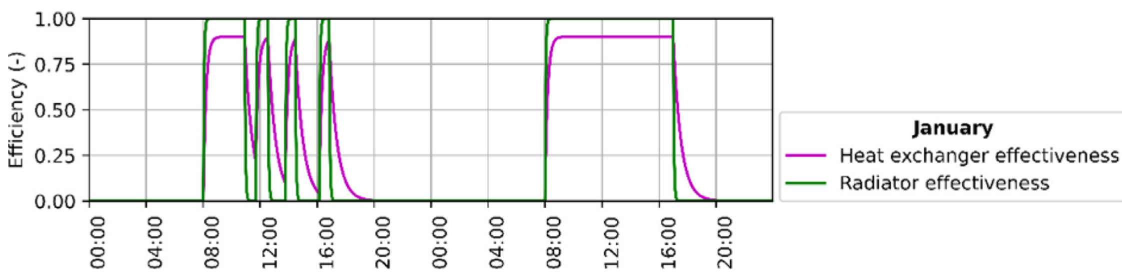

Fig. 3.5. Example of a two-day simulation scenario (effectiveness results of the substation).

fluid. Low temperature levels are also observed in the secondary loop, meaning that the radiator of the consumer operates at lower temperatures than its nominal operation values. This is why the heating capabilities of the substation are effectively reduced.

Moreover, in Figs. 3.4 and 3.5, results regarding the operation of the thermal system can be viewed. To begin with, it is evident that thermal loads are delivered to the building through the substation whenever building internal temperatures drops below setpoint. In addition, the results of the primary mass supply cutdown are displayed in Fig. 3.4, as the thermal power has been significantly reduced during the second day of the simulation. Finally, Fig. 3.5 indicates the effectiveness factors of the substation heat exchanger, as well as the effectiveness of the radiator of the building-consumer. Essentially, variable effectiveness factors indicate the transient thermal phenomena that occur at the moments that heating turns on or off.

3.2. Conventional thermostat cases

In this section the implementation of the parametric simulations will be displayed. To begin with, the conventional thermostat strategy results are displayed in Figs. 3.6 and 3.7. It is noted that the following energy consumption values refer to the second day of the two-day simulation, as that is where the occupancy, as well as the primary flow mass supply reduction take place, as already mentioned.

By observing the thermal comfort levels of Fig. 3.6, it is firstly evident that the heavier the weight category of the building is, the higher the thermal comfort levels are, because of the ability of the heavier structures to retain indoor temperature at higher levels, as more energy has been stored in the opaque elements of the building, from the first day of simulation. Moreover, as expected, as maximum primary loop mass supply cut-down intensifies, thermal comfort drops significantly. This is because the supplied heating power output of the substation is reduced during the second day of the simulation (see Fig. 3.1).

Regarding thermal comfort temperature ranges, the lower ones tend to lead to higher thermal comfort satisfaction. This is because the lower the temperature levels are, the less heating power upkeep is required to maintain them. Therefore, an occupant with thermal comfort zones that reach lower temperatures lead to a building that has higher thermal comfort levels, with that feature being reinforced the heavier the structure is.

What follows is the quantification the maximum mass supply reduction that the building can tolerate without compromising the thermal comfort of the occupant significantly. As already explained in Section 2.1, this limit has been chosen to be the mass supply reduction case where occupant thermal comfort has not dropped more than 5% (e.g., from 90% to 85%), when compared to its respective reference case. The results are displayed in Fig. 3.7.

Results from Fig. 3.7 indicate how thermal comfort changes for each scenario, when exposed to the mass supply reduction event. Each scenario has a maximum primary loop mass supply reduction, which can be viewed in Table 3.1, along with its respective maximum heating power reduction output (derived from Fig. 3.1), without reducing comfort more than 5%.

From Table 3.1 the quantification of maximum flexibility potential through the used indicator, (described in Section 2) is presented, along with the respective maximum substation power output. Without applying a preheating controlling strategy, it can be seen that power output can be reduced by approximately 15% for very light building cases, 17% for medium cases and 30% for heavy cases. Especially in the heavy case, by reducing the thermal comfort zones by 2 °C, the substation potentially is able to change its heating power reduction from 20% to 40%. On the other hand, in the very light case, the respective reduction change is approximately 2%. Moreover, there is a 7% reduction change regarding the medium case. Finally, the mass supply for the same thermal comfort zone change reduces between 30%–60% for all cases. The general remark that comes out of analyzing Table 3.1, the heavier the building is, the more influential the thermal comfort zone change is.

3.3. Preheating thermostat cases

In this section, the preheating strategy scenarios are examined. Due to the purpose of preheating scenarios is to achieve 100%

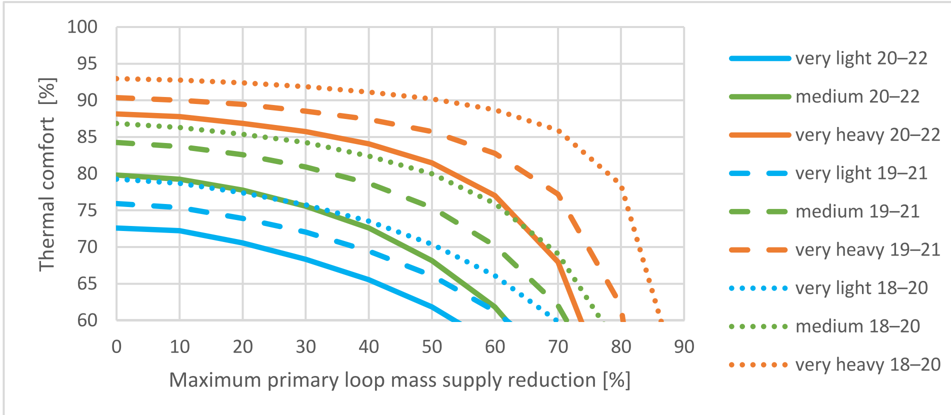

Fig. 3.6. Thermal comfort results for the second simulation day for all conventional heating scenarios.

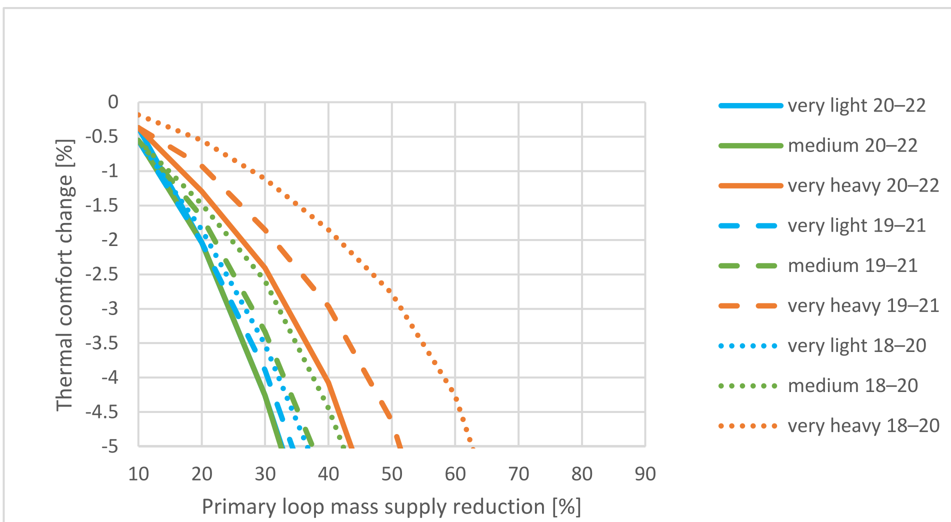

Fig. 3.7. Thermal comfort change results for the second simulation day for all conventional heating scenarios.

Table 3.1
Results of flexibility indicators for all conventional heating scenarios.

Scenario building category	Thermal comfort zone	Maximum primary loop mass supply reduction [%]	Maximum substation power output reduction [%]
Light	20–22	32	14.34
	19–21	34	15.59
	18–20	36	16.84
Medium	20–22	32	14.34
	19–21	37	17.47
	18–20	42	21.07
Heavy	20–22	43	21.94
	19–21	51	28.93
	18–20	63	40.34

thermal comfort, the following figures will contain the preheat time for each scenario instead of thermal comfort levels (Fig. 3.8). That being said, some scenarios of preheating under extreme heat flow reduction did not manage to maximize thermal comfort. More elaborately, those are the scenarios whose preheating time is equal to 15 h (the hours that elapse from 17:00 of the first day to 08:00 of the second day) and maximum comfort has not been attained. Therefore, in those scenarios, further preheating is not allowed, as the preheating schedule overlaps with the conventional heating schedule of the first day.

In Fig. 3.8, the preheating durations are presented for each case. As already mentioned, all cases that reached 15 h of preheating were not able to maximize thermal comfort, and therefore the limit of system flexibility has been surpassed. It can be observed in that some cases, the substation even managed to maximize thermal comfort, even at 90% mass supply reduction, where essentially it operated at four times less power output than the original case (Fig. 3.1), namely 1 kW. Those cases tend to be medium and very heavy cases. However, even in those scenarios, preheat times are large, ranging from 9–13 h approximately. The rest of the cases manage to have their comfort maximized at 80% mass supply reduction, which corresponds to 60% power output reduction.

Regarding thermal comfort ranges, changes in range limits can lead to reduction of the preheating duration in all cases, especially in larger mass supply reduction events. To elaborate, for the very

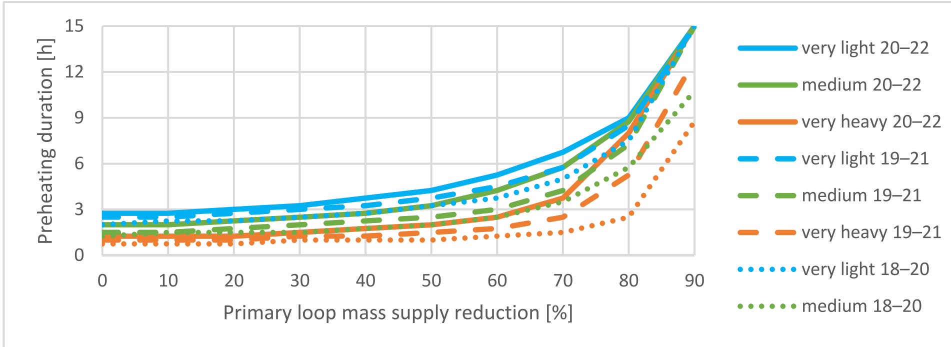

Fig. 3.8. Thermal comfort change results for the second simulation day for all conventional heating scenarios.

light case, a 5%–10% reduction in preheat duration per °C of the zone change. The respective value for the medium case amounts to 17%–20%, while for the very heavy case the reduction amounts to 35%–50%. Moreover, the medium building case is not flexible enough to reduce their mass supply to 90%, when the comfort range is 20-22 °C or 19-21 °C. However, for the case of 18-20 °C comfort case, the medium building manages to achieve maximum thermal comfort when the substation operates at the 10% of the original maximum mass supply, essentially achieving 75% thermal power curtailment.

The results of this approach are now compared with the respective results of other works. First of all, the ways that building weight categories and implemented controlling strategies affect flexibility are similar to observation made by [18,19], which has stated that utilizing the thermal mass, namely preemptively storing heating energy in the thermal mass of the building, in order to cover thermal demands when needed without being impacted by insufficient thermal power. By examining the results of [21], it can be observed that heavier category buildings encourage preheating strategies, which is also confirmed in this work. Finally, the proposed approach has also confirmed the significance of the proposition of recent research [47], namely, to consider thermal comfort settings in the evaluation of the flexibility potential. While the above work has pointed out the impact of the occupant preferences regarding their comfort, this work is also able to provide, with the usage of a performance indicator, a numerical evaluation of how flexible the substation is, towards providing the required thermal loads to the consumer (see Figs. 3.7 and 3.8).

4. Conclusions

To sum up, this work aims at investigating the influence of multiple parameters on the thermal flexibility of a DHN substation. The majority of the explored literature has proposed several approaches for identifying and/or boosting flexibility potential in various cases. Since the aim of flexibility utilization is the reduction of the carbon footprint and the facilitation of RES in the DHN, detailed knowledge of the system flexibility is always crucial. More specifically, an integrated approach is proposed, for estimating maximum flexibility potential in DHNs, during peak shaving events or power supply cutoffs that may occur in a thermal grid. In other words, the purpose of this work is not to provide an optimization methodology for the operation of the substation during peak shaving effects, but rather to demonstrate the contribution of the consideration of thermal comfort settings to the evaluation of the District Heating Network substation flexibility, during peak shaving effects. According to the authors' current knowledge, this is something that has not been examined extensively in the literature, as most works examine flexibility using only the thermal mass and controlling strategies as main factors, which lead to a static evaluation of the flexibility potential. However, this work also proposes a third factor, namely the existing thermal comfort settings of the building, which makes the flexibility evaluation dynamic, at times when thermal comfort settings of consumers also change.

As an example case that implements the proposed methodology, this paper examines and quantifies the maximum thermal flexibility potential of a DHN substation, providing heating loads to a consumer, namely an office building. The parameters that are examined are various building weight categories and thermal comfort zones of the occupant, as well as two different controlling strategy cases. Regarding the first strategy, the building thermostat signals the substation to provide heating loads only during the occupancy periods, only if indoor temperature is lower than the comfort zone. As far as the second strategy is concerned, a smart preheating strategy is adopted, according to which the thermostat calculates the moment that heating loads should be provided before the occupancy period, so that thermal comfort is maximized. A series of dynamic two-day simulations take place, using various combinations of the three parameters mentioned before. In every case scenario, during the first day of the simulation, the building has been heated according to a typical office working schedule. Moreover, in every simulation, the following heating power settings takes place: the substation operates as usual during the first day of the simulation, whereas it is exposed to a heating flow reduction event during the second day of each simulation. The aim of those simulations is to determine the maximum flexibility potential of the substation, namely the maximum heating flow reduction event it can tolerate, without compromising the thermal comfort of the occupant.

According to the results, the three parameters were investigated that affect flexibility potential can be ranked among themselves, in terms of influence on the maximum flexibility potential of the substation. First and foremost, the controlling strategy used (namely in this case the preheating strategy) is the most influential parameter on system maximum power output reduction out of the three, as it managed to raise the flexibility potential of all cases up to at least 60% power output cutdown. The second parameter is the weight category of the building. As it has been observed, heavier buildings possess more flexibility potential, due to the total available thermal mass that can be used to retain indoor temperature levels. Last but not least, an observable impact on maximum flexibility potential is made by taking into account different thermal comfort ranges. What is also worth mentioning is that the importance of taking occupant thermal comfort range into account increases in heavier structures. More specifically, the current work has uncovered that by reducing the thermal comfort zone by 2 °C, the maximum power reduction increased from 15% to 17% for light buildings, and from 30% to 40% in heavy cases. Another remark is that considering thermal comfort ranges also bolsters the influence of preheat controlling strategies. As results displayed in certain building cases where the preheating controlling strategy was in effect, the maximum potential of power output cutdown managed to be increased to from 60 to 75%, just by taking into account the case of lowered thermal comfort settings, that existing approaches usually do not. From the above results, it can be inferred that when seeking the maximum flexibility potential of a substation, considering thermal comfort settings along with thermal mass and implemented controlling strategies can make a significant difference in the evaluation and allows for further exploitation of the flexibility of the district heating network. What is more, since thermal comfort settings vary over the duration of day, the proposed approach is able to capture that variability when evaluating comfort settings.

This approach ultimately can be used in a DHN decision support system, which can be also enriched by a dynamic comfort range inputted by the consumer, as thermal comfort is also considered in the decisions, and therefore inform the consumer about which strategies are suitable to support their thermal comfort requirements. That could lead to a bidirectional exchange of information between producers and consumers, when implementing demand side management procedures in a thermal grid.

That being said, there are limitations to this study that should be addressed. First of all, to support the analysis at this stage, the examined case was limited to a single substation, providing heating loads to a single conditioned zone, while the rest of the DHN was not taken into account during the simulation. Moreover, thermal comfort evaluation was focused on the temperature aspect and, therefore, simplified to an indoor temperature range, in which the occupant felt uniformly comfortable with the indoor environment. Also, other thermal comfort indicators, such as indoor air relative humidity and air velocity, was not considered. Moreover, the evaluation of thermal comfort is based on indoor temperature measurements, whereas other temperatures, such as opaque element temperature should be taken into account as well.

Future work involves the expansion of the refinement of the methodology, by addressing the above limitations. Also, the methodology can be expanded in a larger scale, including several substations and multiple consumers in each substation. Finally, this methodology can be used in a multi-energy approach, which takes advantage of different heat sources.

CRediT authorship contribution statement

Leonidas Zouloumis: Conceptualization, Data curation, Formal analysis, Investigation, Methodology, Software, Validation, Visualization, Writing – original draft. **Nikolaos Ploskas:** Software, Validation, Data curation, Formal analysis, Writing – review & editing. **Giorgos Panaras:** Conceptualization, Funding acquisition, Methodology, Project administration, Resources, Supervision, Writing – review & editing.

Declaration of competing interest

The authors declare that they have no known competing financial interests or personal relationships that could have appeared to influence the work reported in this paper.

Funding

We acknowledge support of this work by the project "Optimization of Kozani District Heating Distribution Network with the use of intelligent systems through operation simulation and optimization of End Consumer Thermal Substations.", financed by The Municipal Enterprise for water supply and sewerage of Kozani (DEYAK).

Data availability

Data will be made available on request

References

[1] Eurostat energy statistics—An overview, 2023, Available online: Energy statistics - an overview - Statistics Explained (europa.eu) (accessed on 24 April 2023).

[2] B. Rezaie, M.A. Rosen, District heating and cooling: Review of technology and potential enhancements, Appl. Energy 93 (2012) 2–10, http://dx.doi.org/10.1016/j.apenergy.2011.04.020.

[3] U. Persson, S. Werner, Heat distribution and the future competitiveness of district heating, Appl. Energy 88 (3) (2011) 568–576, http://dx.doi.org/10.1016/J.APENERGY.2010.09.020.

[4] H. Averfalk, S. Werner, Economic benefits of fourth generation district heating, Energy 193 (2020) http://dx.doi.org/10.1016/j.energy.2019.116727.

[5] S. Werner, International review of district heating and cooling, Energy 137 (2017) 617–631, http://dx.doi.org/10.1016/J.ENERGY.2017.04.045.

[6] H. Lund, P.A. Østergaard, T.B. Nielsen, S. Werner, J.E. Thorsen, O. Gudmundsson, A. Arabkoohsar, B.V. Mathiesen, Perspectives on fourth and fifth generation district heating, Energy 227 (2021) 120520, http://dx.doi.org/10.1016/j.energy.2021.120520.

[7] M. Bilardo, F. Sandrone, G. Zanzottera, E. Fabrizio, Modelling a fifth-generation bidirectional low temperature district heating and cooling (5GDHC) network for nearly zero energy district (nZED), Energy Rep. 7 (2021) 8390–8405, http://dx.doi.org/10.1016/J.EGYR.2021.04.054.

[8] D. Connolly, H. Lund, B.V. Mathiesen, S. Werner, B. Möller, U. Persson, T. Boermans, D. Trier, P.A. Østergaard, S. Nielsen, Heat roadmap europe: Combining district heating with heat savings to decarbonise the EU energy system, Energy Policy 65 (2014) 475–489, http://dx.doi.org/10.1016/J.ENPOL.2013.10.035.

[9] E. Guelpa, G. Mutani, V. Todeschi, V. Verda, Reduction of CO2 emissions in urban areas through optimal expansion of existing district heating networks, J. Clean. Prod. 204 (2018) 117–129, http://dx.doi.org/10.1016/j.jclepro.2018.08.272.

[10] I. del Hoyo Arce, S.H. López, S.L. Perez, M. Rämä, K. Klobut, J.A. Febres, Models for fast modelling of district heating and cooling networks, Renew. Sustain. Energy Rev. 82 (2018) 1863–1873, http://dx.doi.org/10.1016/j.rser.2017.06.109.

[11] H. Cai, C. Ziras, S. You, R. Li, K. Honoré, H.W. Bindner, Demand side management in urban district heating networks, Appl. Energy 230 (2018) 506–518, http://dx.doi.org/10.1016/J.APENERGY.2018.08.105.

[12] E. Guelpa, L. Marincioni, S. Deputato, M. Capone, S. Amelio, E. Pochettino, V. Verda, Demand side management in district heating networks: A real application, Energy 182 (2019) 433–442, http://dx.doi.org/10.1016/J.ENERGY.2019.05.131.

[13] R. Bessa, C. Moreira, B. Silva, M. Matos, Handling renewable energy variability and uncertainty in power systems operation, Wiley Interdiscip. Rev. Energy Environ. 3 (2) (2014) 156–178, http://dx.doi.org/10.1002/wene.76.

[14] A. Vandermeulen, B. van der Heijde, L. Helsen, Controlling district heating and cooling networks to unlock flexibility: A review, Energy 151 (2018) 103–115, http://dx.doi.org/10.1016/j.energy.2018.03.034.

[15] G. Reynders, R. Amaral Lopes, A. Marszal-Pomianowska, D. Aelenei, J. Martins, D. Saelens, Energy flexible buildings: An evaluation of definitions and quantification methodologies applied to thermal storage, Energy Build. 166 (2018) 372–390, http://dx.doi.org/10.1016/J.ENBUILD.2018.02.040.

[16] R.A. Lopes, A. Chambel, J. Neves, D. Aelenei, J. Martins, A literature review of methodologies used to assess the energy flexibility of buildings, Energy Procedia 91 (2016) 1053–1058, http://dx.doi.org/10.1016/j.egypro.2016.06.274.

[17] J. Clauz, C. Finck, P. Vogler-Finck, P. Beagon, Control strategies for building energy systems to unlock demand side flexibility – a review, in: 12th International Conference of IBPSA (Building Simulation 2017) San Francisco, US, 2017, https://www.researchgate.net/publication/324877113.

[18] K. Johansen, H. Johra, A niche technique overlooked in the danish district heating sector? Exploring socio-technical perspectives of short-term thermal energy storage for building energy flexibility, Energy 256 (2022) http://dx.doi.org/10.1016/j.energy.2022.124075.

[19] J. le Dréau, P. Heiselberg, Energy flexibility of residential buildings using short term heat storage in the thermal mass, Energy 111 (2016) 991–1002, http://dx.doi.org/10.1016/J.ENERGY.2016.05.076.

[20] J. Bravo Dias, G. Carrilho da Graça, Using building thermal mass energy storage to offset temporary BIPV output reductions due to passing clouds in an office building, Build. Environ. 207 (2022) 108504, http://dx.doi.org/10.1016/J.BUILDENV.2021.108504.

[21] J. Vivian, D. Quaggiotto, A. Zarrella, Increasing the energy flexibility of existing district heating networks through flow rate variations, Appl. Energy 275 (2020) http://dx.doi.org/10.1016/J.APENERGY.2020.115411.

[22] T.Q. Péan, J. Salom, R. Costa-Castelló, Review of control strategies for improving the energy flexibility provided by heat pump systems in buildings, J. Process Control 74 (2019) 35–49, http://dx.doi.org/10.1016/j.jprocont.2018.03.006.
[23] L.M.P. Ghilardi, A.F. Castelli, L. Moretti, M. Morini, E. Martelli, Co-optimization of multi-energy system operation, district heating/cooling network and thermal comfort management for buildings, Appl. Energy 302 (2021) 117480, http://dx.doi.org/10.1016/J.APENERGY.2021.117480.
[24] Y. Wang, S. You, H. Zhang, W. Zheng, X. Zheng, Q. Miao, Hydraulic performance optimization of meshed district heating network with multiple heat sources, Energy 126 (2017) 603–621, http://dx.doi.org/10.1016/j.energy.2017.03.044.
[25] M. di Somma, B. Yan, N. Bianco, G. Graditi, P.B. Luh, L. Mongibello, V. Naso, Multi-objective design optimization of distributed energy systems through cost and exergy assessments, Appl. Energy 204 (2017) 1299–1316, http://dx.doi.org/10.1016/J.APENERGY.2017.03.105.
[26] E. Guelpa, A. Bischi, V. Verda, M. Chertkov, H. Lund, Towards future infrastructures for sustainable multi-energy systems: A review, Energy 184 (2019) 2–21, http://dx.doi.org/10.1016/J.ENERGY.2019.05.057.
[27] D.F. Dominković, P. Gianniou, M. Münster, A. Heller, C. Rode, Utilizing thermal building mass for storage in district heating systems: Combined building level simulations and system level optimization, Energy 153 (2018) 949–966, http://dx.doi.org/10.1016/j.energy.2018.04.093.
[28] K. Foteinaki, R. Li, T. Péan, C. Rode, J. Salom, Evaluation of energy flexibility of low-energy residential buildings connected to district heating, Energy Build. 213 (2020) 109804, http://dx.doi.org/10.1016/J.ENBUILD.2020.109804.
[29] C. Saletti, N. Zimmerman, M. Morini, K. Kyprianidis, A. Gambarotta, A control-oriented scalable model for demand side management in district heating aggregated communities, Appl. Therm. Eng. 201 (2022) http://dx.doi.org/10.1016/j.applthermaleng.2021.117681.
[30] E. Saloux, J.A. Candanedo, Model-based predictive control to minimize primary energy use in a solar district heating system with seasonal thermal energy storage, Appl. Energy 291 (2021) 116840, http://dx.doi.org/10.1016/j.apenergy.2021.116840.
[31] A. de Lorenzi, A. Gambarotta, M. Morini, M. Rossi, C. Saletti, Setup and testing of smart controllers for small-scale district heating networks: An integrated framework, Energy 205 (2020) http://dx.doi.org/10.1016/j.energy.2020.118054.
[32] N. Zimmerman, K. Kyprianidis, C.F. Lindberg, Achieving lower district heating network temperatures using feed-forward MPC, Materials 12 (15) (2019) http://dx.doi.org/10.3390/ma12152465.
[33] W. Birk, K.T. Atta, F. Uden, Improving district heating system operation through control configuration selection and adaptive control, in: 2019 18th European Control Conference, ECC 2019, 2019, pp. 2944–2949, http://dx.doi.org/10.23919/ECC.2019.8795742.
[34] B. Zhang, A.M.Y.M. Ghias, Z. Chen, A double-deck deep reinforcement learning-based energy dispatch strategy for an integrated electricity and district heating system embedded with thermal inertial and operational flexibility, Energy Rep. 8 (2022) 15067–15080, http://dx.doi.org/10.1016/J.EGYR.2022.11.028.
[35] T. Fang, R. Lahdelma, Genetic optimization of multi-plant heat production in district heating networks, Appl. Energy 159 (2015) 610–619, http://dx.doi.org/10.1016/j.apenergy.2015.09.027.
[36] M. Kouhia, T. Laukkanen, H. Holmberg, P. Ahtila, District heat network as a short-term energy storage, Energy 177 (2019) 293–303, http://dx.doi.org/10.1016/j.energy.2019.04.082.
[37] M. Leśko, W. Bujalski, K. Futyma, Operational optimization in district heating systems with the use of thermal energy storage, Energy 165 (2018) 902–915, http://dx.doi.org/10.1016/j.energy.2018.09.141.
[38] E. Guelpa, Impact of thermal masses on the peak load in district heating systems, Energy 214 (2021) http://dx.doi.org/10.1016/j.energy.2020.118849.
[39] E. Guelpa, G. Barbero, A. Sciacovelli, V. Verda, Peak-shaving in district heating systems through optimal management of the thermal request of buildings, Energy 137 (2017) 706–714, http://dx.doi.org/10.1016/j.energy.2017.06.107.
[40] T. Van Oevelen, L. Scapino, J. al. Koussa, D. Vanhoudt, A case study on using district heating network flexibility for thermal load shifting, Energy Rep. 7 (2021) 1–8, http://dx.doi.org/10.1016/j.egyr.2021.09.061.
[41] K.M. Luc, R. Li, L. Xu, T.R. Nielsen, J.L.M. Hensen, Energy flexibility potential of a small district connected to a district heating system, Energy Build. 225 (2020) http://dx.doi.org/10.1016/J.ENBUILD.2020.110074.
[42] X. Yang, L. Pan, W. Guan, H. Ma, C. Zhang, Heat flexibility evaluation and multi-objective optimized control of a low-energy building with district heating, Energy Build. 277 (2022) http://dx.doi.org/10.1016/j.enbuild.2022.112523.
[43] S. Huo, J. Wang, Y. Qin, Z. Cui, Operation optimization of district heating network under typical modes for improving the economic and flexibility performances of integrated energy system, Energy Convers. Manage. 267 (2022) 115904, http://dx.doi.org/10.1016/J.ENCONMAN.2022.115904.
[44] L. Chen, S. Jin, G. Bu, Experimental investigation of a novel multi-tank thermal energy storage system for solar-powered air conditioning, Appl. Therm. Eng. 123 (2017) 953–962, http://dx.doi.org/10.1016/J.APPLTHERMALENG.2017.05.160.
[45] M. Turski, R. Sekret, Buildings and a district heating network as thermal energy storages in the district heating system, Energy Build. 179 (2018) 49–56, http://dx.doi.org/10.1016/J.ENBUILD.2018.09.015.
[46] M. Frontczak, P. Wargocki, Literature survey on how different factors influence human comfort in indoor environments, Build. Environ. 46 (4) (2011) 922–937, http://dx.doi.org/10.1016/j.buildenv.2010.10.021.
[47] S. Martinez, M. Vellei, J. le Dréau, Demand-side flexibility in a residential district: What are the main sources of uncertainty? 2021, http://dx.doi.org/10.1016/j.enbuild.2021.111595.
[48] Greek Technical Chamber, Technical Directive 20701-3: Climatic Data for Greek Areas, Athens, 2010.
[49] S.A. Klein, W.A. Beckman, TRNSYS 16: A transient system simulation program: mathematical reference, in: TRNSYS, Vol. 5, 2007, pp. 389–396.
[50] International Standard Organization, ISO 13790-2008, Energy Performance of Buildings, Calculation of Energy Use for Space Heating and Cooling, ISO, Geneva, Switzerland, 2008.
[51] I. Ballarini, A. Costantino, E. Fabrizio, V. Corrado, The dynamic model of EN ISO 52016-1 for the energy assessment of buildings compared to simplified and detailed simulation methods, in: Building Simulation Conference Proceedings, Vol. 6, 2019, pp. 3847–3854, http://dx.doi.org/10.26868/25222708.2019.210431.
[52] J.A. Duffie, W.A. Beckman, N. Blair, Solar Engineering of Thermal Processes, Photovoltaics and Wind, fifth ed., Wiley, 2020.
[53] L. Zouloumis, G. Panaras, Development of a smart thermostat, in: IAQ 2020: Indoor Environmental Quality Performance Approaches, 2021.